CHAPTER 6
HANDHELD ANTENNA ARRAY TESTBED (HAAT)

6.1 Introduction

An experiment system was developed to measure diversity combining and adaptive beamforming performance using various array configurations and combining algorithms. This chapter describes the Handheld Antenna Array Testbed (HAAT) system and associated hardware and software. The HAAT was developed based on the requirements of planned antenna diversity and adaptive beamforming experiments. Key features of this system include portability and ability to test hand-held antenna configurations in typical microcellular and peer-to-peer communication scenarios.

This chapter begins with an overview of the HAAT system, followed by descriptions of the system components. The components include transmitters, a linear positioning system, two- and four-channel receivers and data loggers, data processing hardware, and the software used to process data and evaluate performance of diversity combining and adaptive beamforming. Sample graphs of the data processing software outputs are shown.

6.2 System Overview

A high-level block diagram of the HAAT is shown in Fig. 6-1. The HAAT operates at 2.05 GHz. CW signals are transmitted from one or two transmitters. Data are collected using either a two- or a four-channel portable receiver system. The data are analyzed off line to allow comparison of different combining techniques. Figure 6-2 shows the two-channel receiver/data logger and data processing system. Each of the components of the HAAT is described in this section. More details on the software are included in the Appendices.

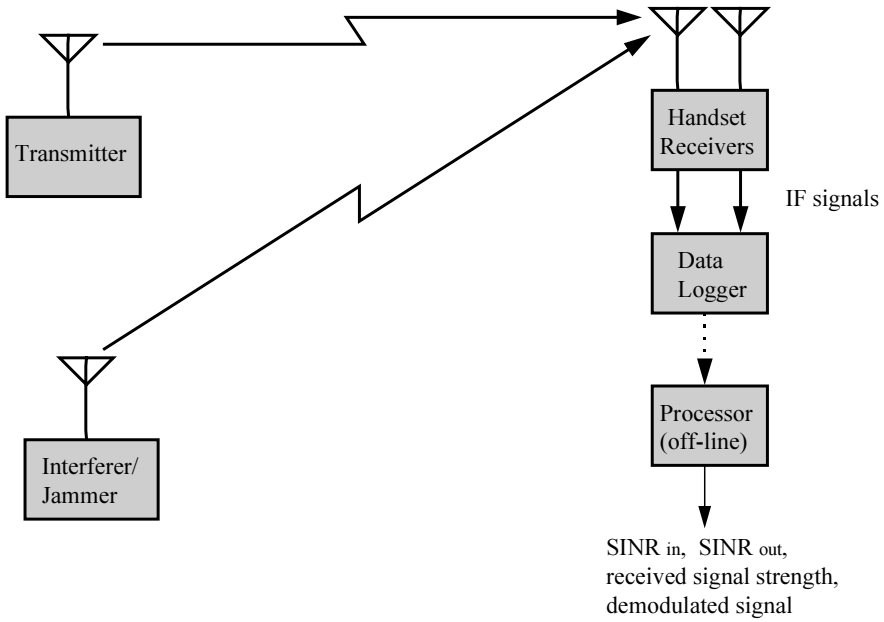

Figure 6-1. High level system block diagram of the Handheld Antenna Array Testbed (HAAT).

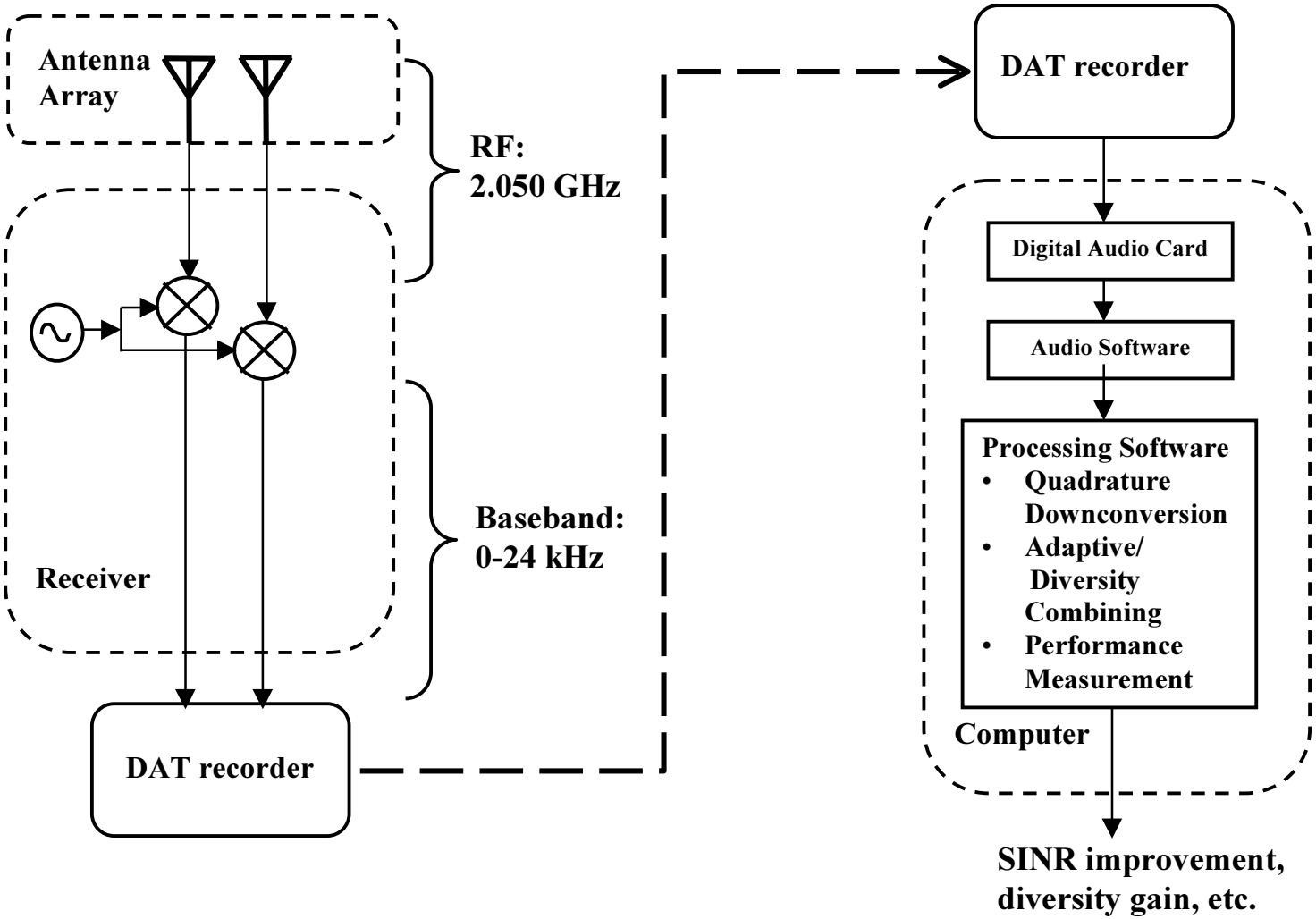

Figure 6-2. Block diagram of the two-channel HAAT receiver/data logger and data processing system

6.3 Transmitters

The testbed uses one or two transmitters. For diversity measurements only one of the transmitters is used. Both transmitters are used when interference rejection measurements are performed to evaluate adaptive beamforming performance. Either source can be considered as transmitting the desired signal. The other source is then an interfering signal. The transmitters use the architecture depicted in Fig. 6-3. Table 6-1 lists the major transmitter components. The transmitters are typically mounted on tripods and operate from fixed positions but are transportable and run on batteries for use in the field. Additional transmitters can be added as needed. The transmitters transmit continuous wave (CW) signals at 2.05 GHz. The transmitter frequencies are offset by about 1 kHz so that the signals can be distinguished, and both signals fall within the bandwidth of the receiver unit.

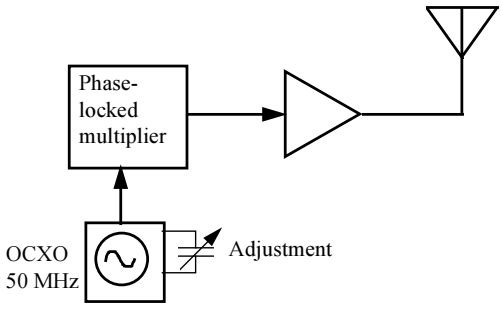

Figure 6-3. Block diagram of a HAAT transmitter

Table 6-1. Major Transmitter Components

Component	Manufacturer	Part Number	Quantity per Transmitter
Reference Oscillator	Hewlett Packard		1
Signal Source	NOVA SOURCE	20002500-100X	1
Power Amplifier	MINI CIRCUITS	ZFL 2500 VH	1
Batteries (6V gel cells)	Power Patrol	SLA0905	3

6.4 Linear Positioning System

A portable positioning system is used for controlled measurements. The positioning system is shown in Fig. 6-4 and consists of a non-metallic track approximately 3 m in length. The major positioner components are listed in Table 6-2.

The useable length of the track is about 2.8 m (approximately 20 wavelengths at 2.05 GHz). The receiver is mounted on a carriage that is moved along the track at a constant speed, using a stepper motor, while measurements are conducted. The track is mounted on an adjustable tripod to allow use on any terrain. An electronic level is used to adjust the tripod to level the track.

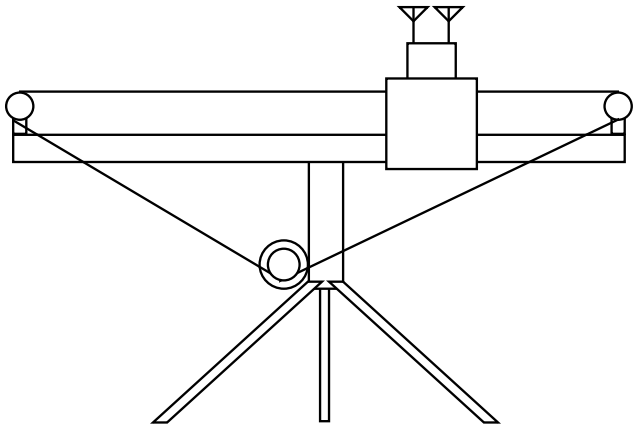

Figure 6-4. Positioning system for controlled tests

Table 6-2. Major Positioning System Components

Component	Manufacturer	Part Number	Quantity
Motor	Superior Electric	M061-FD-427U	1
Motor Controller	J. R. Nealy		1
Motor Controller Board	Modern Technology	MTSD-V1	1
Battery (6V gel cell)	Power Patrol	SLA0905	1
Tripod			1
Track	J. R. Nealy		1
Carriage	J. R. Nealy		1

6.5 Two-Channel Handheld Receiver Unit and Data Logger

The handheld receiver unit consists of a box having the approximate size and shape of a handheld radio and includes antennas, receivers, and a portable DAT recorder (a Sony TCD-D8), used to log data. Two antennas, each connected to a separate receiver, are mounted on the box. The receiver IF outputs are connected to the DAT. The entire receiver unit is portable so that it can be carried by an operator, and is rugged enough that it can be used to perform experiments in a wide variety of locations and conditions.

Figure 6-5 shows the receiver and data logger. The received RF signals are mixed down to baseband and recorded on the two channels of a digital audiotape (DAT) recorder. The recorder is capable of recording at 32,000, 44,100, and 48,000 samples per second for a maximum 24 kHz bandwidth. For the experiments reported here, the 32 kHz sampling rate was used to minimize the size of the data files. The components of the two-channel HAAT receiver are listed in Table 6-3.

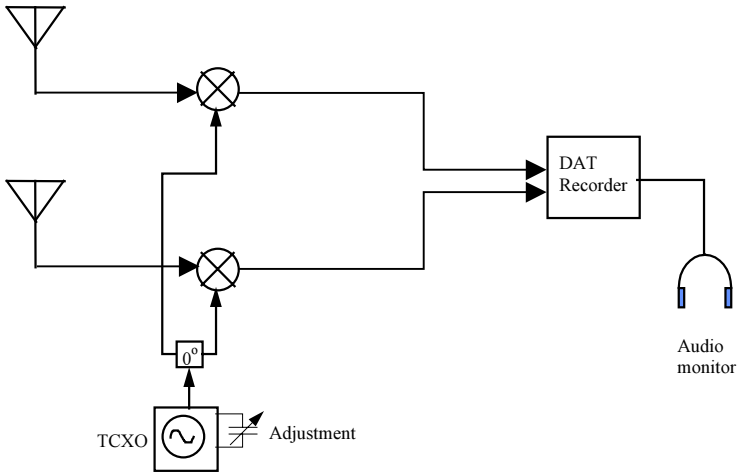

Figure 6-5. Receiver architecture block diagram.

Table 6-3. Major Two-Channel Receiver Components

Component	**Manufacturer**	**Part Number**	**Quantity**
Bandpass Filter	CIRQTEL	A-102-587	2
Mixer	MINI CIRCUITS	ADE-18@	2
Local Oscillator	NOVA ENGR.	20002500-100	1
0° Splitter	MINI CIRCUITS	LRPS-2-25	1
Lowpass Filter	SONY (built into DAT recorder)	None	2

The noise floor of the two-channel receiver was measured to be –88 dBm. The link budget for the receiver is shown in Table 6-4. The transmit-receive range was calculated for a variety of propagation conditions. Because the receiver was used to measure fading signal envelopes, fade margins of 10 to 30 dB were used in the link budget calculations.

Table 6-4. Link Budget for the Two-Channel HAAT Receiver

Transmitter power, dBm	27.00	27.00	27.00
Transmitter cable losses, dB	2.00	2.00	2.00
Gain of transmitting antenna, dBi	2.15	2.15	2.15
EIRP, dBm	27.15	27.15	27.15
Gain of receiving antenna, dBi	2.15	2.15	2.15
Receiver cable losses, dB	2.00	2.00	2.00
Receiver noise floor, dBm	-88.00	-88.00	-88.00
Minimum mean SNR (fade margin), dB	10.00	20.00	30.00
Maximum allowable path loss, dB	105.30	95.30	85.30
Wavelength in m at 2.05 GHz	0.1463	0.1463	0.1463
Path loss in dB at 1 m, 2.05 GHz	38.7	38.7	38.7
Maximum path loss beyond 1m	66.6	56.6	46.6
Maximum range in m, free space, n=2	**2144**	**678**	**214**
Maximum range in m, n=3	**166**	**77**	**36**
Maximum range in m, n=4	**46**	**26**	**15**

6.6 Four-Channel HAAT Receiver and Data Logger

Figure 6-6 shows a block diagram of the 4-channel receiver, as well as a high-level view of the data collection and processing. Each antenna is connected directly to a mixer and the received RF signal at 2.05 GHz is mixed down directly to baseband. Filtering is performed by the anti-aliasing filters internal to the two portable digital audio tape machines that are used to record the data. This configuration results in low power consumption. The noise figure of 28 dB is relatively high but suitable for the application. The receiver is powered by three lead-acid gel-cell batteries that supply 18 V DC. The receiver draws approximately 200 mA.

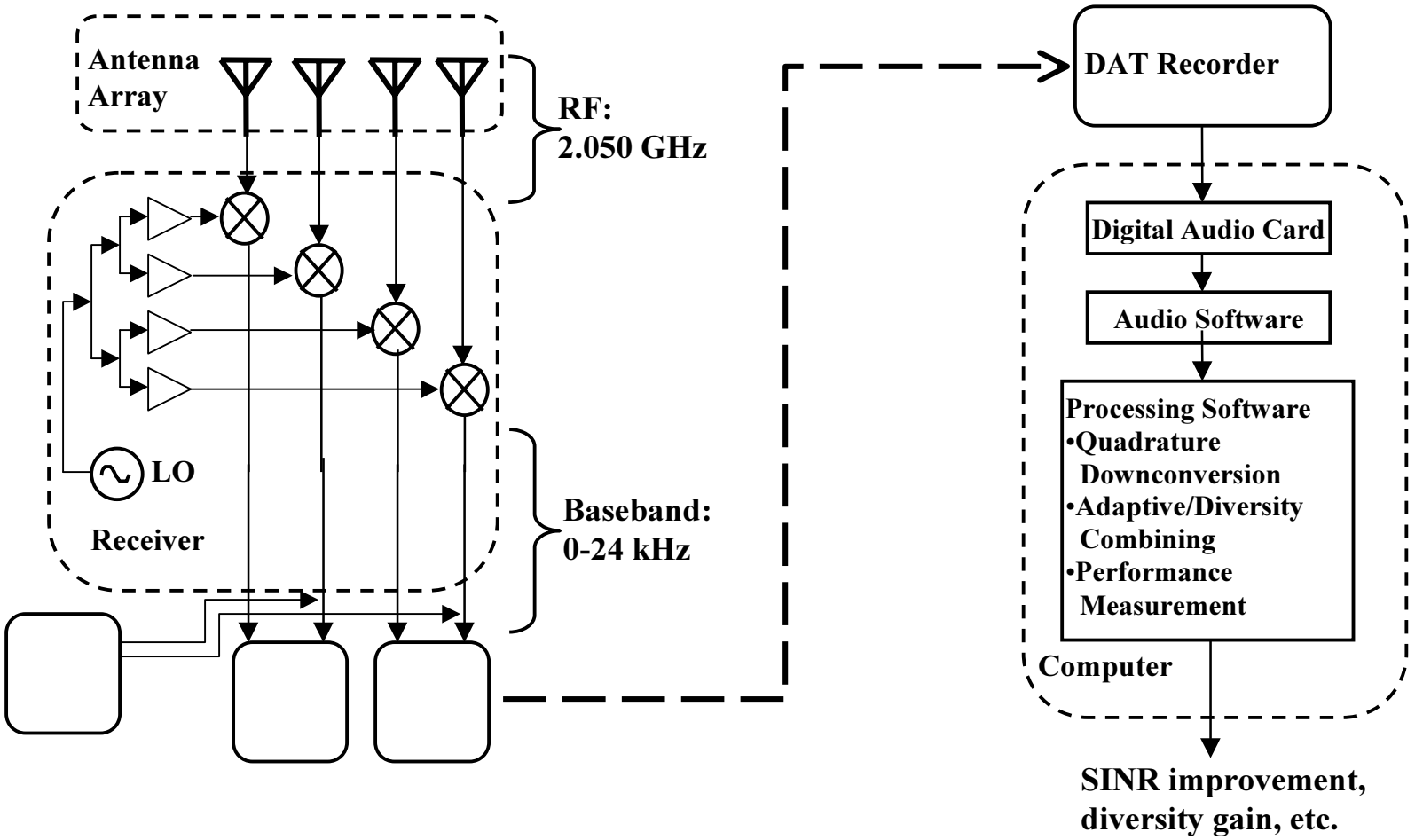

Figure 6-6. Block diagram of the 4-channel HAAT receiver

6.6.1 Calibration of the four-channel receiver

The receiver was calibrated using the configuration shown in Fig. 6-7. An HP 8648C signal generator was connected to two channels of the receiver using a two way splitter. The signal generator was set to a frequency of 2.05 GHz and the output power was varied from –130 to –30 dBm (resulting in -134 to –34 dBm into the receiver). The two unused antenna ports were terminated in 50 Ωloads. The received signal was recorded on a DAT as in normal operation of the receiver

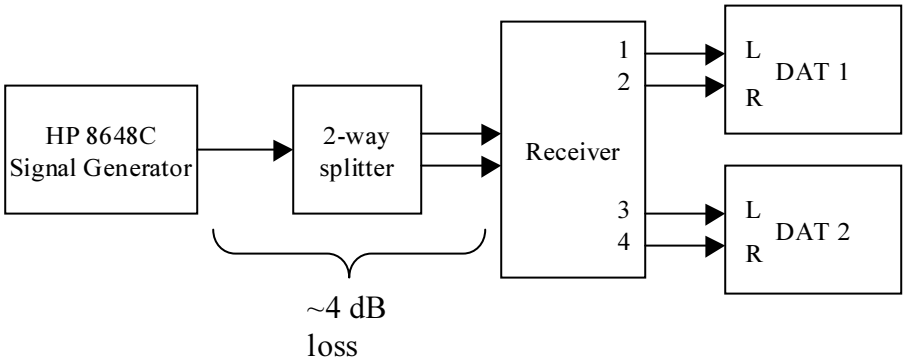

Figure 6-7. Block diagram of the equipment configuration used for receiver calibration.

The noise floor was calculated using the relative total signal-plus-noise power in measurements with a known signal power. The noise floor was calculated using the diversity combining software and was found to be –126 dBm in a 100 Hz bandwidth.

When using the adaptive beamforming software, the noise floor was determined by the mean measured ratio of the power in the 100 Hz signal bandwidth (due to a known input power) to the power in 100 Hz bandwidth at a frequency a few kHz removed from the received signal. This is a close approximation of signal-to-noise ratio (SNR) and depends on the length of the window used in the calculation. The noise floor was found to be approximately
–122 dBm with a window of 320 samples and –125 dBm for a window of 640 samples.

The maximum power that did not overload the DAT was –36 dBm. Combined with the noise floor measurements, this yields a dynamic range for the receiver of between 86 and 90 dB, depending on the software that is used. This is in line with the claimed dynamic range of 87+ dB for the digital audiotape recorder. This indicates that quantization noise and not thermal noise is the dominant noise source in this receiver. Using the diversity combining software, the noise figure of the receiver was calculated to

be 28 dB, but the receiver would have to be measured directly without using the DAT recorder in order to calculate the noise figure accurately.

The usable dynamic range of the system is limited by the need to detect synchronization pulses that are used to mark the beginning and end of each measurement. This problem is described in more detail later in this section. In addition, the phase noise due to the local oscillators in the transmitter and receiver, measured at 1kHz from the spectral peak, is relatively high at approximately 54 dB below the peak signal power. This limits the maximum signal-to-interference-plus-noise ratio (SINR) that can be measured to approximately 54 dB.

A link budget was calculated using the measured noise floor and a distance-dependent exponential path loss model. The link budget, shown in Table 6-4, includes a fade margin of 10 to 50 dB to allow measurement of fading of the received signal or signals. Also, the maximum interference rejection that can be measured is determined by the fade margin.

Table 6-4. Link budget for the 4-channel HAAT receiver

Transmitter power, dBm	27.00	27.00	27.00	27.00	27.00
Transmitter cable losses, dB	1.00	1.00	1.00	1.00	1.00
Gain of transmitting antenna, dBi	2.15	2.15	2.15	2.15	2.15
EIRP, dBm	28.15	28.15	28.15	28.15	28.15
Gain of receiving antenna, dBi	2.15	2.15	2.15	2.15	2.15
Receiver cable losses, dB	1.00	1.00	1.00	1.00	1.00
Receiver noise floor, dBm	-122.00	-122.00	-122.00	-122.00	-122.00
Minimum mean SNR (fade margin), dB	**10.00**	**20.00**	**30.00**	**40.00**	**50.00**
Maximum allowable path loss, dB	141.30	131.30	121.30	111.30	101.30
Wavelength in m at 2.05 GHz	0.1463	0.1463	0.1463	0.1463	0.1463
Path loss in dB at 1 m, 2.05 GHz	38.7	38.7	38.7	38.7	38.7
Maximum path loss beyond 1m	102.6	92.6	82.6	72.6	62.6
Maximum range in m, n=2 (free space)	**135256**	**42772**	**13526**	**4277**	**1353**
Maximum range in m, n=3	**2635**	**1223**	**568**	**263**	**122**
Maximum range in m, n=4	**368**	**207**	**116**	**65**	**37**

Additional measurements were performed to calibrate the receiver for phase and power balance between channels. Measurements were performed similar to those for the noise floor calculations. The signal generator was adjusted to provide a signal first at a frequency close to that of the first HAAT transmitter (4 kHz offset from the receiver LO) and then at a frequency close to that of the second HAAT transmitter (5 kHz offset from

the receiver LO). A power level of –74 dBm, well within the linear range of the receiver, was used. Two channels were sampled at the same time. First, channels 1 and 2 were measured, then channels 1 and 3, then 1 and 4. For each pair of channels, two measurements were taken at each frequency. The cable connections to the two receiver ports were switched between measurements to calibrate out phase and power imbalances in the splitter. The results are shown in Table 6-5.

Table 6.5 Power and Phase Balance Between Channels of the 4-channel HAAT Receiver.

Amplitude and Phase Balance	Amp bal., dB	Phase bal., degrees
Ch 2/ Ch 1, 4kHz	-0.15	-9.34
Ch 2/ Ch 1, 5kHz	-0.15	-9.36
Ch 3/ Ch 1, 4kHz	0.08	9.45
Ch 3/ Ch 1, 5kHz	0.09	9.44
Ch 4/ Ch 1, 4kHz	0.07	9.08
Ch 4/ Ch 1, 5kHz	0.06	9.05

In typical operation of the HAAT, synchronization pulses are inserted in the receiver baseband output at the beginning and end of each measurement. The pulses have two purposes. First, they mark the beginning and end of a measurement. If the positioner is used, the pulses mark the beginning and end of the receiver's motion. Second, the pulses allow synchronization of data collected with two different DAT recorders, where each DAT records two of the four channels of the receiver. The pulses are generated by coupling the switch from the HAAT positioner motor controller to the receiver audio output for channels 2 and 4. The resistor values in the circuit were selected so that the starting pulse was approximately 3 dB below the maximum input level to the DAT. The ending pulse was approximately 10 dB lower than the starting pulse. This results in a maximum input signal level of approximately –40 dBm if the starting pulse is to be detected, or –50 dBm if both pulses are to be detected. The effective dynamic range of the receiver is reduced to about 72 dB in the latter case. Mean synchronization error is defined as

$$\varepsilon_{synch} = \frac{|n_1 - n_2|}{\min(n_1, n_2)} \quad \text{[unitless (samples/sample)]} \tag{6.1}$$

where n_1 is the number of samples recorded on tape 1 in a specific measurement (marked by beginning and ending pulses) and n_2 is the number of samples recorded on tape 2 during the measurement.

For measurements using the positioner, the total time is approximately 24 seconds and the mean synchronization error is ε_{synch}=20x10^{-6} to 25x10^{-6}. For longer measurements ε_{synch} is lower. From these measurements it is not possible to determine the maximum value of ε_{synch} during a given measurement

6.7 Data Processing Hardware

The HAAT data processing system is used to analyze the collected data. The system consists of a computer with an interface to the data logger and software that determines statistics of the collected data and can be used to determine the performance of different combining techniques for each antenna configuration tested. The system uses a 450 MHz Pentium II computer with 256 MB of RAM that runs Windows NT 4.0 Workstation. A Digital Audio Laboratories Digital Only CardD^{TM} is used to interface with a Sony DTC-700 DAT recorder that is used to play back the recorded data.

6.8 Data Processing Software

Data are recorded onto the hard disk of the computer using Sonic Foundry's SoundForge XP 4.0 software. Data are stored in Microsoft wave file format, using a sampling rate of 32, 44.1, or 48 kHz, 2 channels, 16 bits per sample. In this format one minute of data at 32,000 samples per second occupies approximately 10 MB of disk space. A large (10.1 GB) hard disk drive was used to store the data, permitting a maximum of over 1000 minutes of recorded data to be stored. The "defrag" program was run periodically to ensure that disk space is used efficiently. This is necessary so that available space on the hard drive can be accessed quickly enough to record the data in real time.

The data processing software is implemented in MATLAB 5.0. The software reads the data from wave files and processes the data to determine the statistics of the data and the performance of combining techniques. The HAAT data processing software evaluates diversity combining based on diversity gain and also evaluates adaptive beamforming performance based on SINR improvement. The software allows several

parameters to be varied. Additional data processing software can be written as needed. Details on quantification of diversity and adaptive beamforming performance are found in Appendix.A

6.8.1 Diversity combining evaluation software

Each measurement is processed individually and then each set of measurements is processed to calculate statistics for a particular measurement location. Diagrams of the processing software are shown in Fig. 6-8 (a) and (b), respectively. Each individual measurement (data from a single run of the receiver down the track) is processed in two steps as shown in Fig. 6-8 (a). The raw data from each diversity measurement are stored in a wave (.wav) file. The program "divproc" reads the wave file and calculates the mean branch powers, normalized and/or demeaned sampled branch envelopes, and envelope correlations, and writes these data in a pre-processed (*.div) file. Divproc uses a diversity update rate and demeaning window supplied by the user. The program "divdisplay" reads the data from the pre-processed data file and calculates the mean and mean absolute branch power imbalance, level crossing rates, and diversity gain for maximal ratio, equal gain, and selection techniques. Level crossing rates are calculated for 0, -10, -20, -30, and -40 dB relative to the mean of the stronger branch. All these data are stored in a structure called dddata and written to a processed data (*.ddd) file. Divdisplay can display the branch envelopes before and after combining, and the cumulative distribution functions of the envelopes before and after combining, with diversity gain, power imbalance, and envelope correlation information, and the best fit Ricean fading distribution for each channel. Diversity gain was calculated from the envelopes of the branch signals. This was found to give nearly identical results to diversity gain calculations using direct measurement of the SNR. Details of the calculations are given in the Appendix.

Measurement sets are processed based on information contained in a measurement set description file with extension .ddf. This file contains a structure called divdata that contains an output file name and directory and a list of processed data files from individual measurements that are to be processed as part of the set. The structure also contains information on the antenna spacing used for each measurement, and descriptions of the antenna configuration, type of channel, location, and date of the

measurement set. The program “divstats” reads the measurement set description file and the measurement processed data files specified in the measurement set description file, and calculates statistics for each antenna spacing used in the measurement set. The calculated statistics are stored in a structure called pdivdata that also contains the information on the measurement set from the divdata structure, and the pdivdata structure is written to a processed measurement set data file named *.pdd. The calculated statistics include the mean of the envelope correlation, the mean absolute power imbalance, the mean power imbalance, the mean level crossing rates before and after combining, and the mean diversity gain for measurements using each antenna spacing.

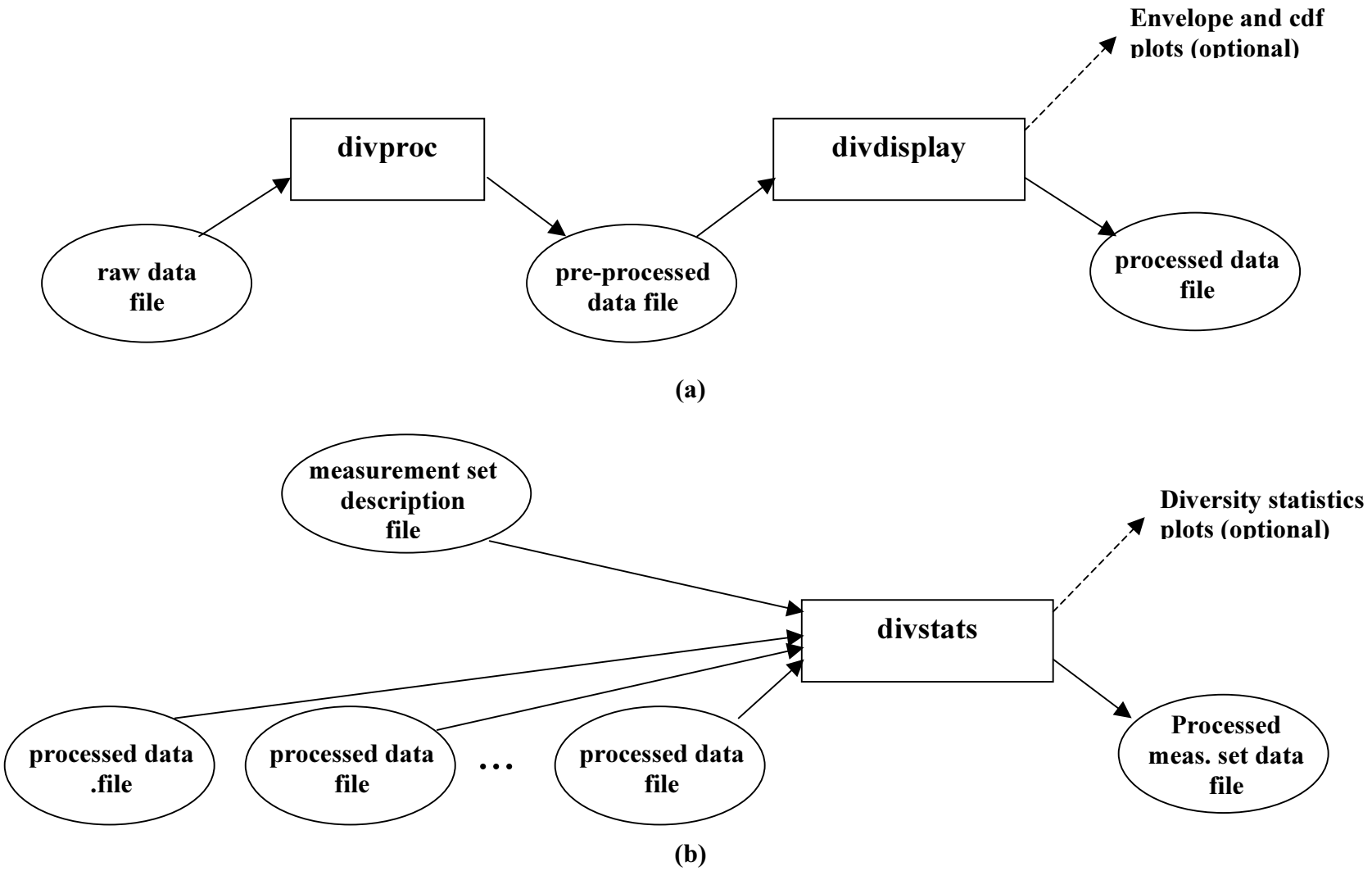

Figure 6-8. Data processing software modules for diversity measurements: (a) for each measurement, (b) for measurement se

6.8.1.1 Demeaning

Variations in the received signal envelope are caused by fast fading due to multipath and also by shadowing (slow fading) due to obstructions in the channel. An operational system must contend with both fast and slow fading. Power control can compensate for large changes in shadowing, but some variation due to shadowing, which is correlated for closely spaced antennas, will persist depending on the power control implementation.

For comparison with the theory developed for fast fading channels, it is desirable to remove the effects of shadowing from the data. This is accomplished by demeaning which is performed by dividing the instantaneous envelope by the *local mean* of the envelope. The local mean is found as follows [2], [25]:

$$m(x) = \frac{1}{2L}\int_{x-L}^{x+L} A_0(\tau)d\tau \text{ [volts]} \qquad (6.2)$$

where x is position and $2L$ is the demeaning window (x and L can be measured in any units of distance, e.g., meters or wavelengths), and A_0 is the envelope, in volts. The envelope is then viewed as consisting of the local mean and a *fast-fading component* $A(x)$ as follows:

$$A_0(x) = m(x)A(x) \text{ [volts]} \qquad (6.3)$$

One way to determine the length of the demeaning window to use is to find a window that is just long enough to substantially eliminate the effects on the local mean of nulls in the instantaneous envelope, and that yields high correlation between the local means of the two channels. Figure 6-9 shows the local means for a measurement in an urban, non line-of-sight channel in which the receiver was moved over 19 wavelengths. The signal envelopes shown were demeaned using windows of $2L$ = 1 to 6λ in increments of 1λ. Rapid fluctuations in the local mean become less evident as the demeaning window is increased. The correlations of the local means are shown in Table 6-6. In general, there are not large variations in the local mean over a few wavelengths, so demeaning is not needed for short measurements.

For measurements taken over long distances, the local mean can change by 20 dB or more, and demeaning is necessary to measure the performance of diversity combining accurately. Figure 6-10 shows the signal envelope from a long indoor non line-of-sight

measurement. The envelope without demeaning is shown in Fig. 6-10 (a). The local mean changes by about 60 dB over the course of the measurement. The local mean is nearly constant after demeaning with a window of $2L \approx 19\text{m} \approx 130\lambda$, as shown in Fig. 6-10 (b).

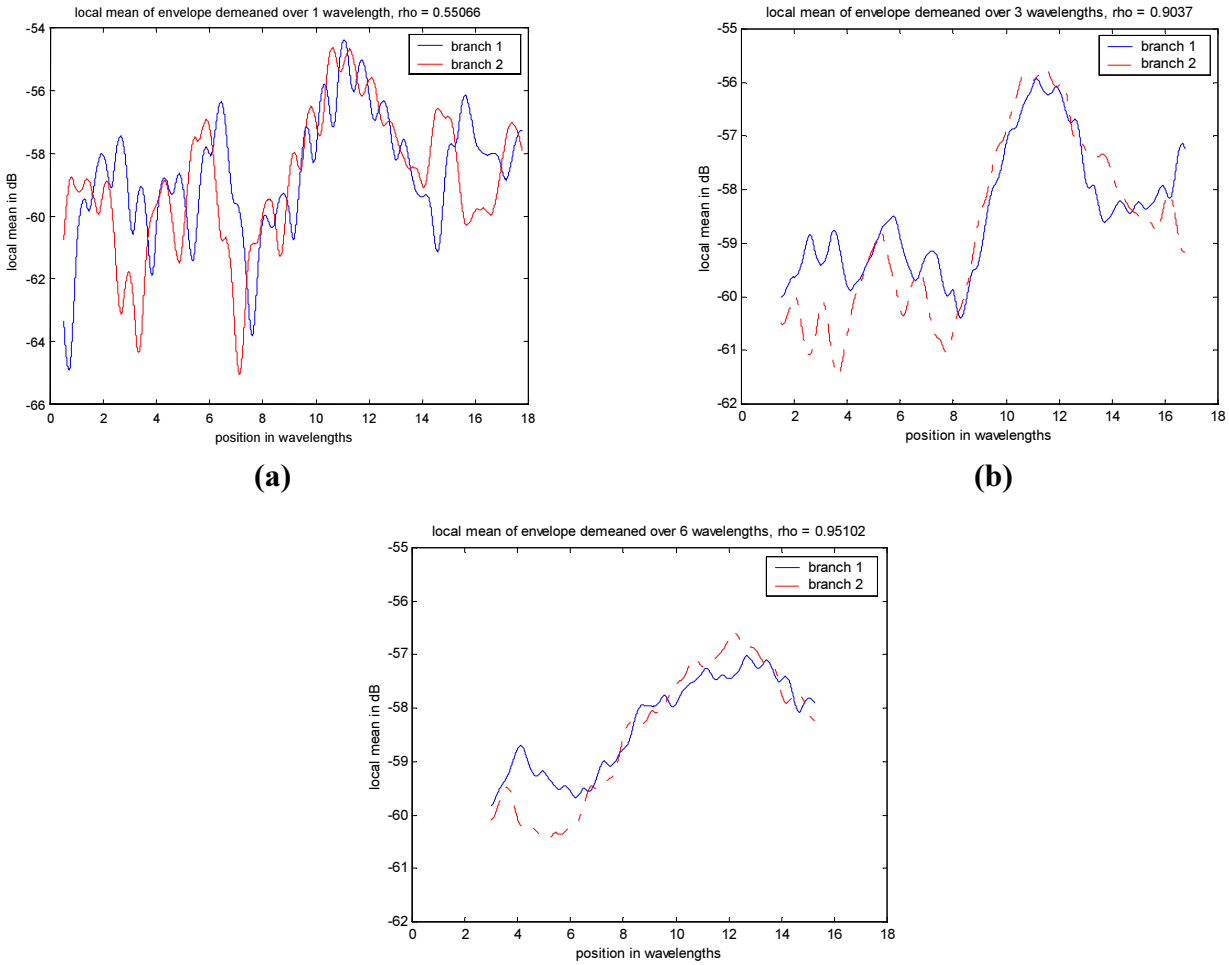

Figure 6-9. Local means of measured envelopes in urban, non line-of-sight channel for different demeaning window lengths $2L$: (a) $2L=\lambda$, (b) $2L=3\lambda$, (c) $2L=6\lambda$

Table 6-6. Correlation of local means of envelopes for different demeaning windows

Demeaning window 2*L* in wavelengths	**Correlation of local means, ρ_{lm}**
1	0.55
2	0.78
3	0.90
4	0.95
5	0.95
6	0.95

6.8.1.2 Normalization of branch envelopes

As stated in the introduction, power balance is important for determining the diversity gain of a system. It is essential that this information is not lost in the data processing. To accomplish this, the instantaneous envelopes of both branches are divided by the local mean of the stronger branch. When processing the data without demeaning, both envelopes are normalized by the overall mean of the stronger branch. This approach yields envelopes that are normalized relative to a common reference and preserves the power balance information, which would be lost if the branches were demeaned independently. Figure 6-10 shows measured signal envelopes in an urban, non line-of-sight channel, without demeaning and with demeaning using a three-wavelength window. Note that demeaning significantly reduces variation in the peaks of the envelope.

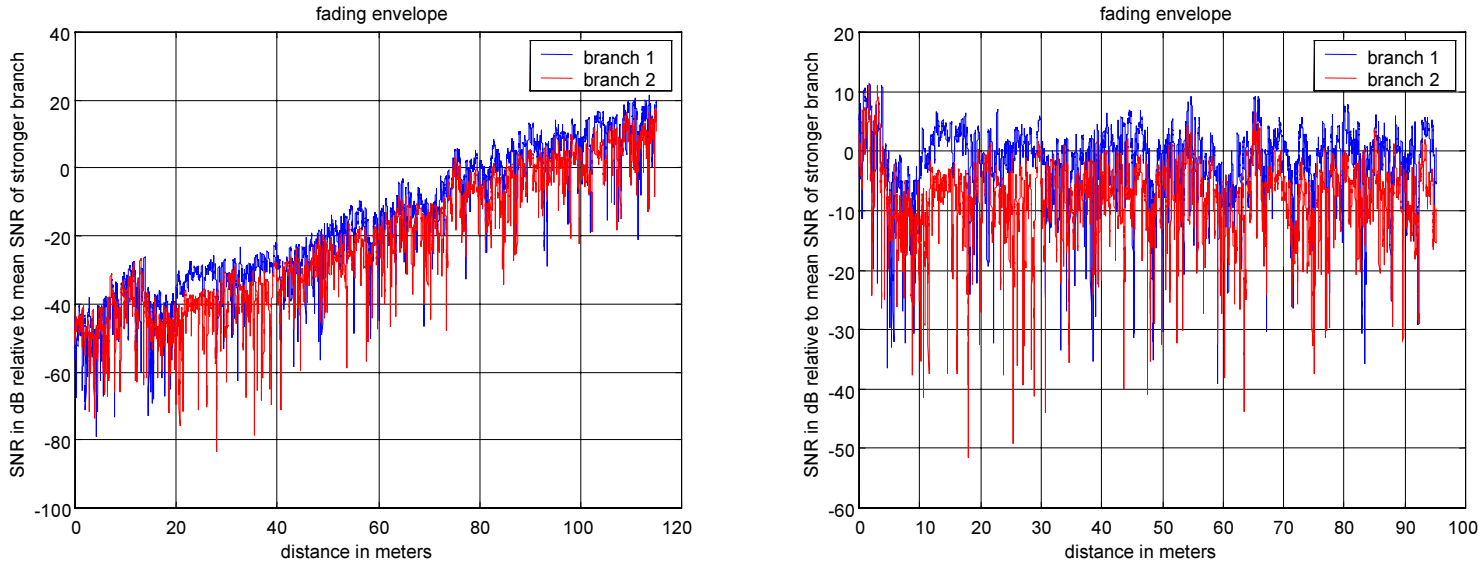

Figure 6-10. Signal envelopes vs. position in an indoor, non line-of-sight channel: (a) without demeaning, (b) with demeaning using a window of length ($2I \approx 130\lambda$)

6.8.1.3 Ricean CDF curve fit

The probability distribution of the envelope in a fading channel can be characterized by a Ricean distribution. For each measurement, the Ricean parameter K (the specular-to-random power ratio) is found that yields a best fit to the normalized cdf of the measured envelope for each channel. K is expressed as a ratio and not in dB in the curve-fitting process. K is varied in increments of 0.1 and the value of K that minimizes mean squared error between the theoretical and measured cdfs becomes the estimated specular-to-random power for the channel. A channel that has only multipath with no dominant path will have a value of K=0 (Rayleigh fading). An example of a best fit Ricean CDF for an urban non line-of-sight channel is shown in Fig. 6-11, where K was found to be approximately 1.5 or 1.8 dB. This corresponds to the theoretical fading distribution for a received signal with one dominant component that has approximately 1.5 times the total power of all the other multipath components. Knowledge of the fading distribution allows us to determine whether the measured diversity gain should be expected to approach the theoretical diversity gain for Rayleigh fading.

6.8.1.4 Diversity gain

Diversity gain was calculated as described in the Appendix. In Fig. 12, CDFs are shown in Fig. 6-12 for the envelopes of the signals received by each diversity branch, as well as for the calculated envelope of the signal after maximal ratio combining. This particular experiment was performed in a non line-of-sight urban channel and used an antenna spacing of $d=0.5\lambda$. The CDFs are normalized to the time average SNR of the stronger branch. The diversity gain for a given cumulative probability (read from the y-axis) is the horizontal distance between the curve for the stronger branch (channel 1 in this case) and the curve for the combined signal. For example, the diversity gain from Fig. 6-12 is approximately 6.7 dB for 10% cumulative probability and 11.6 dB for a 1% cumulative probability. That is, diversity gain equals or exceeds 6.7 dB 10% of the time and exceeds 11.6 dB 1% of the time.

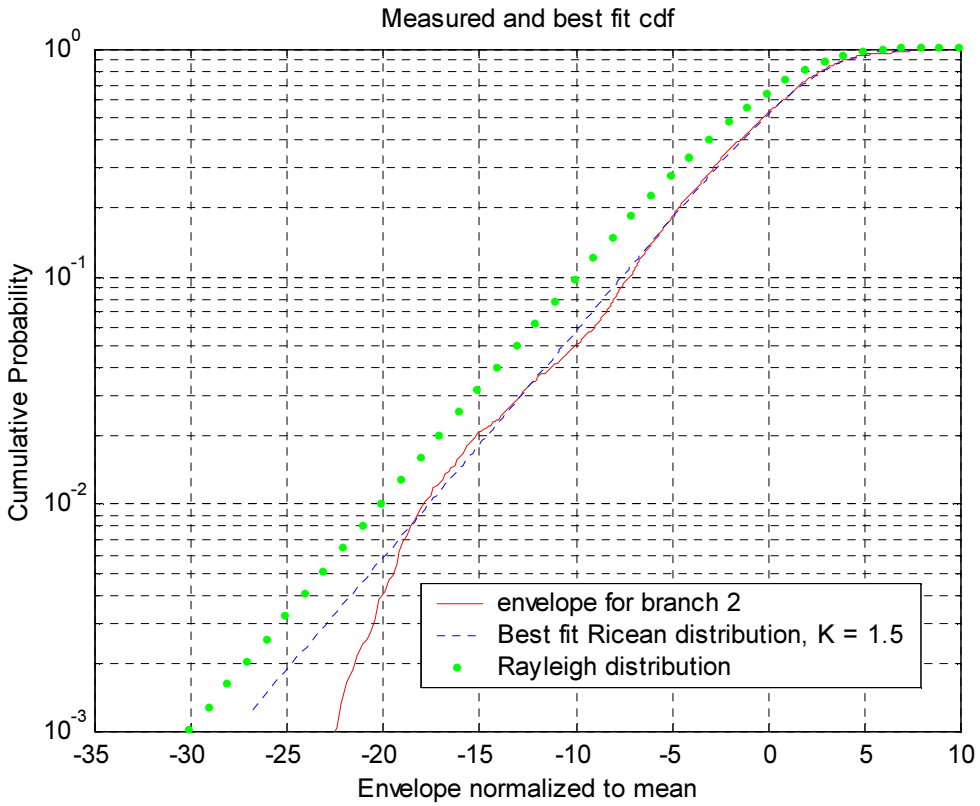

Figure 6-11 . CDF of signal envelope with best fit Ricean CDF, *K*=1.5.

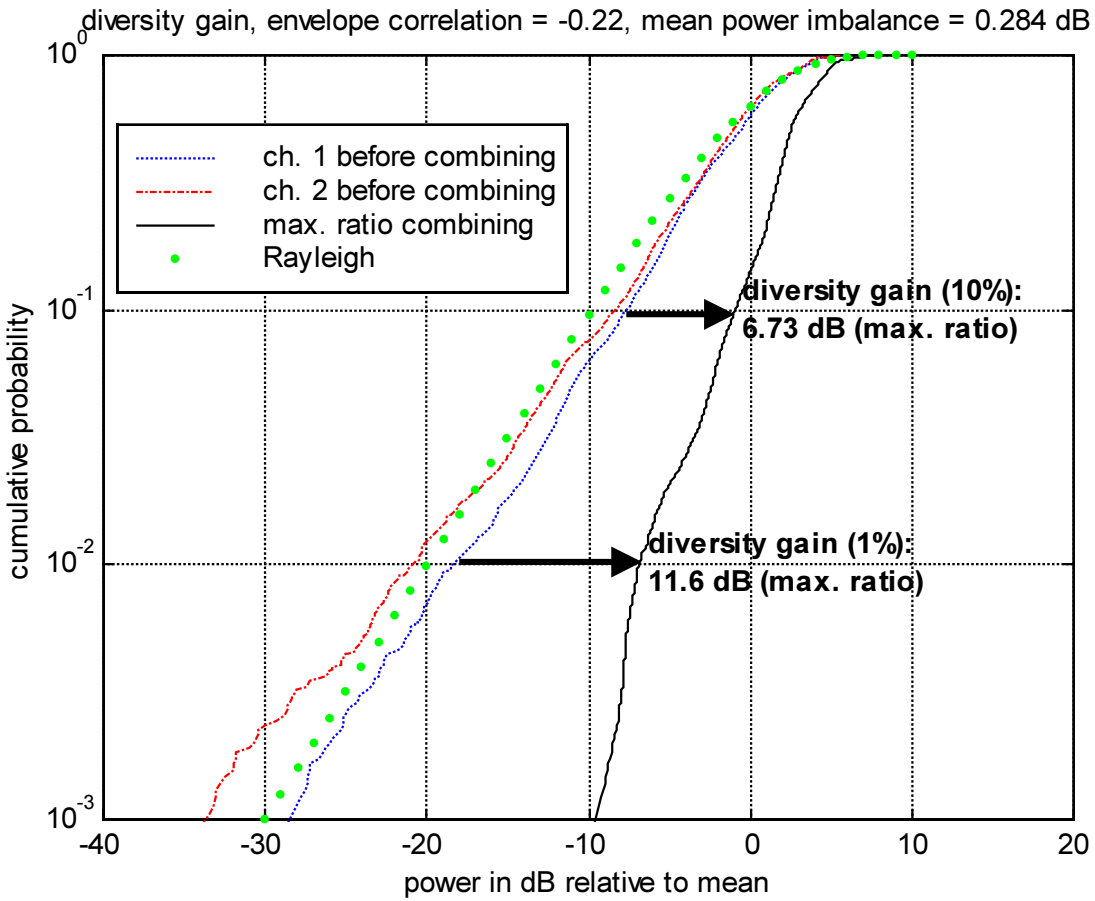

Figure 6-12. Cumulative distribution function of signals before and after diversity combining, showing diversity gain, for an urban, non line-of-sight measurement with antenna spacing d=0.5λ.

6.8.2 Adaptive beamforming evaluation software

Each adaptive beamforming measurement is processed and then each set of adaptive beamforming measurements is processed as shown in Fig. 6-13 (a) and (b), respectively. Each individual measurement is processed in two steps as shown in Fig. 6-13 (a). The raw data from each 4-channel adaptive beamforming measurement are stored in two wave (.wav) files. The program "cmaproc4" reads the wave files and calculates the signal to interference-plus-noise ratio (SINR), signal to noise ratio (SNR), and synchronization error, and writes these data in a pre-processed (*.cma) file.

The program cmaproc4 uses several parameters that are specified by the user. These include the block length used in the constant modulus algorithm, the block length used to calculate SINR, the interval between orthogonalization of weights in the multi-target algorithm, the number of algorithm iterations per block, the bandwidth to be used in SINR and SNR calculations, and the name to be given to the pre-processed file. SINR is calculated as follows. The FFT of the first second of data is calculated and the two frequency bins that have the highest power are identified. For each data block of the specified size, the SINR is calculated as the ratio of power in the bins in a specified bandwidth about the frequency of the signal of interest to the power in the bins in the same bandwidth about the frequency of the other signal. The SNR for each block is calculated by dividing the power in the bins near the frequency of the signal of interest by the power in an equivalent bandwidth about a baseband frequency of 7 kHz.

The program cmadisplay4 reads the data from the pre-processed (*.cma) data file, and calculates and displays the mean SINR and SNR, and SINR and SNR for 10%, 1%, and 0.1% cumulative probabilities. These data are stored in a structure called dabdata and written to a processed data (*.dab) file. The program cmadisplay4 displays the SINR and SNR vs. time, before and after combining, and the cumulative distribution functions of the SINR and SNR. It also estimates the upper limit on possible SINR. This estimate is equal to the sum of the mean SNRs on each of the receiver branches and represents the mean SNR that would be achieved using maximal-ratio diversity combining in the absence of interference.

Measurement sets, which consist of several measurement runs using different antenna configurations and positioner angles, are processed based on information

contained in a measurement set description file with extension .abf. This file contains a structure called abfdata that contains an output file name and directory and a list of processed data files from individual measurements that are to be processed as part of the set. The structure also contains information on the antenna spacing used for each measurement, and descriptions of the antenna configuration, type of channel, location, and date of the measurement set. The program "abfstats" reads the measurement set description file and the processed data files for each measurement specified in the measurement set description file, and calculates statistics for each measurement case used in the measurement set. The calculated statistics are stored in a structure called pabdata that also contains the information on the measurement set from the abfdata structure, and the pab structure is written to a processed measurement set data file named *.pab. The calculated statistics include the following for each measurement: the mean SINR and SINR at cumulative probabilities of 10%, 1%, and 0.1% for each signal before and after beamforming, and the synchronization error.

A sample plot of SINR vs. time is shown in Fig. 6-14 (a) and a plot of the CDF of SINR is shown in Fig. 6-14 (b). In Fig. 6-14 (a) there are large variations in the SINR before beamforming, due to multipath fading in both the desired and interfering signals. The SINR after beamforming fluctuates rapidly but does not have large excursions. In this measurement the mean SINR after beamforming is within about 2 dB of the estimated value of 45.4 dB. Figure 6-14(b) shows the cumulative probability vs. SINR. For example, for a cumulative probability of 10^{-2} or 1%, the SINR after beamforming, shown by the solid line, is 31.4 dB. This is the SINR level that is exceeded 99% of the time. By locating the dashed lines at the same cumulative probability level, it can be seen that, at this cumulative probability level, the CMA algorithm has achieved an improvement of 42 dB over the SINR measured on any of the four branches before beamforming.

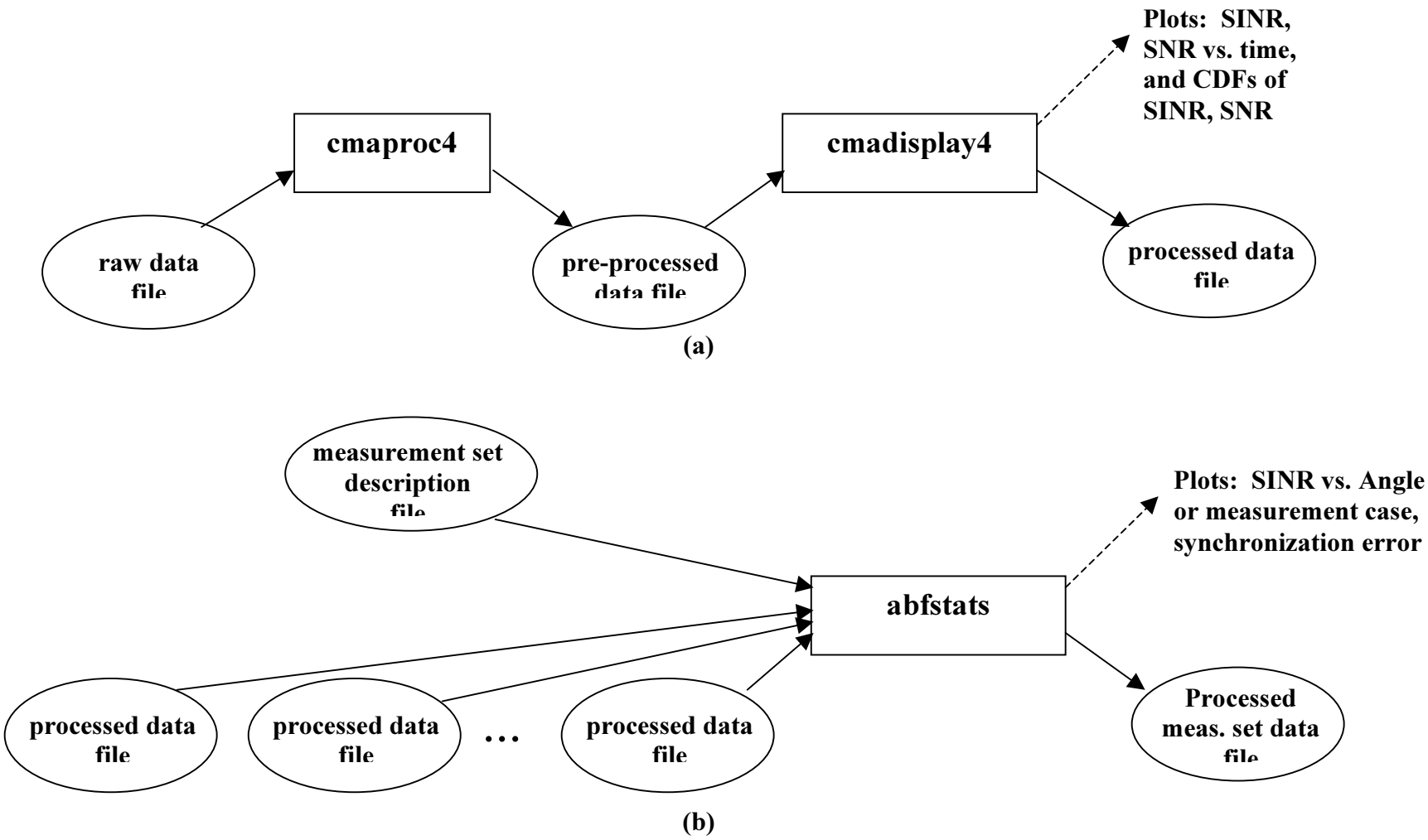

Figure 6-13. Data processing software modules for adaptive beamforming measurements:
(a) for individual measurement, (b) for measurement set.

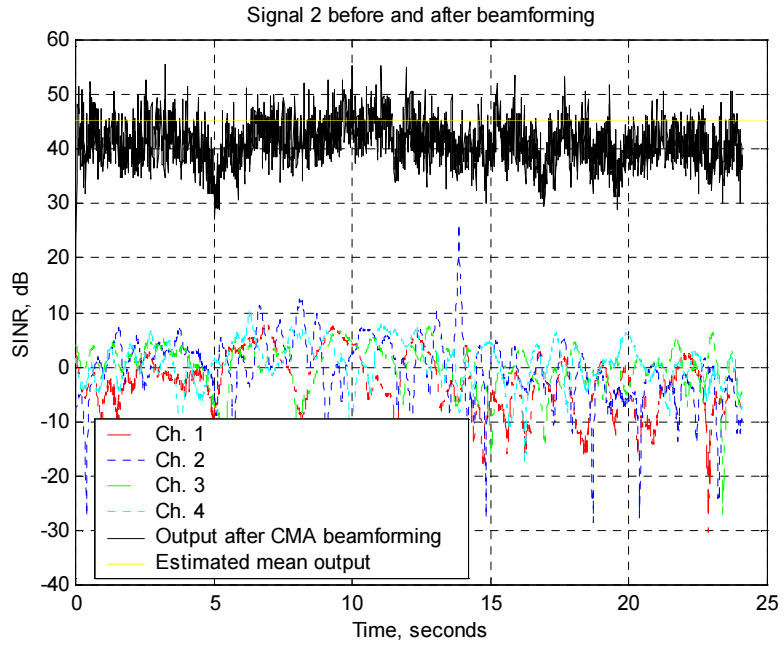

(a)

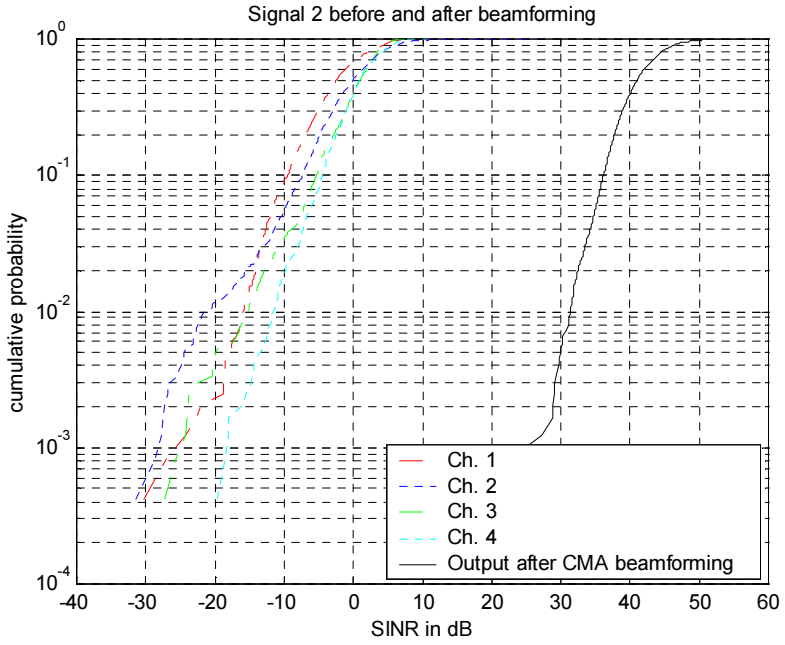

(b)

Figure 6-14. Plots of SINR from adaptive beamforming measurements: (a) SINR vs. time, (b) cumulative probability of SINR.

For measurement cases in which there is no interference, the least-squares constant modulus algorithm (LSCMA), described in Chapter 3, provides diversity gain against fading because it tends to maintain the envelope of the beamformer output at a nearly constant level. To test the adaptive beamforming evaluation software, the diversity gain achieved using LSCMA was compared to the calculated diversity gain for maximal ratio combining. The adaptive beamforming software (cmaproc4 and cmadisplay4 shown in Fig. 6-13) was used to process some of the data from measurements that had previously been processed using the diversity combining evaluation software described in Section 6.8.1. The SNR after beamforming with the LSCMA was calculated and the diversity gain using this algorithm was also calculated. Results for an urban, non line-of-sight measurement are shown in Fig. 6-15.

Figure 6-15 (a) shows the results obtained for maximal ratio combining. It shows cumulative probability as a function of SNR normalized to the mean SNR of the stronger of the two branch signals, before processing. The cumulative probability distribution of the calculated SNR for a maximal ratio combiner with a 500 Hz update rate is also plotted. The horizontal difference between the two curves is the diversity gain in dB, which is a function of the cumulative probability. The cumulative probability distributions of the SNRs of the two branch signals and of the output signal after processing with the LSCMA (with the weights updated 100 times per second) are shown in Fig. 6-15 (b). The diversity gain achieved by the LSCMA beamformer is shown in Fig. 6-15 (b). As is expected, the agreement in diversity gains between the LSCMA and maximal-ratio combining is very good. Maximal ratio combining provides diversity gains of $G_{div,mr}$=6.7 dB at the 10% cumulative probability level and $G_{div,mr}$=11.6 dB at the 1% cumulative probability level. The diversity gains measured for the LSCMA beamformer are $G_{div,LSCMA}$=6.3 dB at 10% cumulative probability and $G_{div,LSCMA}$=12.4 dB at 1% cumulative probability. Agreement below the 1% level is not as close, probably because the maximal ratio combining output SNR was calculated based on the input SNR using a faster update rate than that used by the LSCMA beamformer.

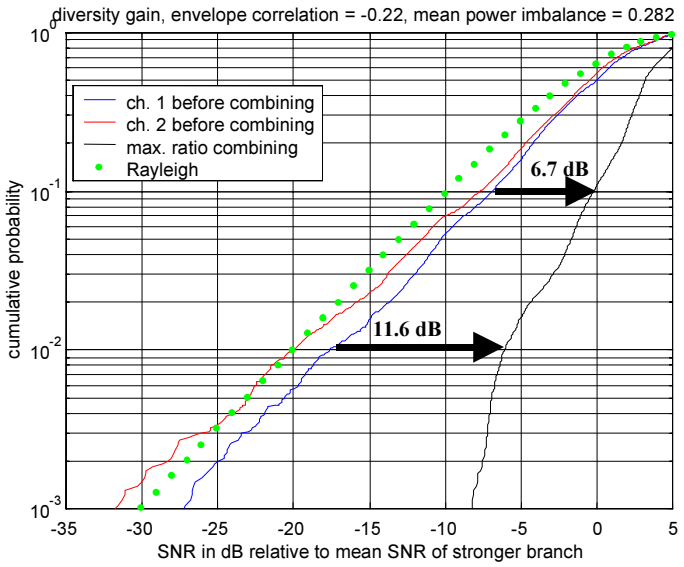

(a)

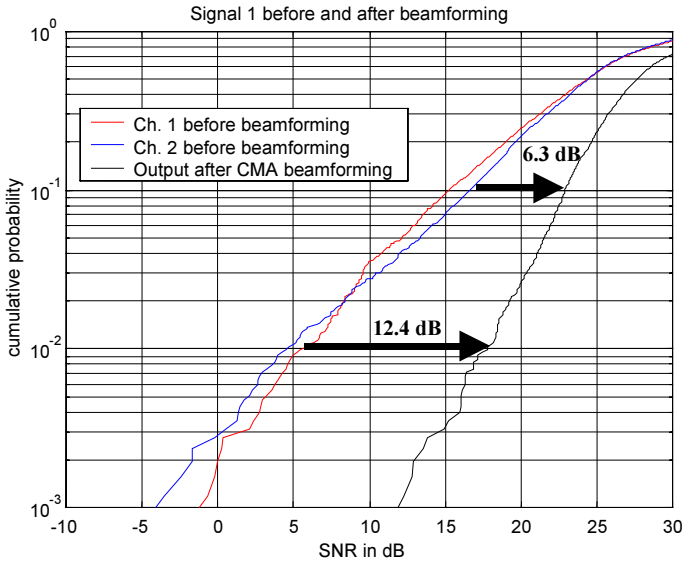

(b)

Figure 6-15. Cumulative probability distributions showing diversity gain for: (a) maximal ratio combining and (b) LSCMA beamformer.

6.9 Conclusions

This chapter described the Handheld Antenna Array Testbed (HAAT) and its hardware and software components. The HAAT consists of a portable narrowband RF measurement system that operates at 2.05 GHz and data processing hardware and software. The HAAT allows quantitative evaluation of diversity combining and adaptive

beamforming using various array configurations and combining algorithms. The system supports controlled measurements using a linear positioner to move the receiver and measurements in which the receiver is carried by an operator as in typical handheld radio operation. Two- and four-channel receiver and data logger units were constructed and system link budgets were calculated based on the performance of each receiver. A single transmitter is used in experiments that measure the effectiveness of diversity combining to mitigate fading, and two transmitters are used in experiments that measure the effectiveness of adaptive beamforming to reject interference. The data processing software quantifies the performance of diversity combining or adaptive beamforming, to facilitate comparison of different antenna configurations.